

Supplementary material for

## Zinc borate glasses: properties, structure and modelling of the composition-dependence of borate speciation

Brian Topper<sup>1,2\*</sup>, Doris Möncke<sup>1</sup>, Randall E. Youngman<sup>3</sup>, Christina Valvi<sup>4</sup>, Efstratios I. Kamitsos<sup>5</sup>, Christos P.E. Varsamis<sup>4\*</sup>

<sup>1</sup> *Inamori School of Engineering at the New York State College of Ceramics, Alfred University, 1 Saxon Drive, Alfred, NY 14802, USA*

<sup>2</sup> *Department of Physics & Astronomy and Center for High Technology Materials, University of New Mexico, Albuquerque, NM 87131, USA*

<sup>3</sup> *Science and Technology Division, Corning Incorporated, Corning, New York 14831, USA*

<sup>4</sup> *Applied Physics Laboratory, Faculty of Engineering, University of West Attica, 250 Thivon, 112 41 Egaleo, Attica, Greece*

<sup>5</sup> *Theoretical and Physical Chemistry Institute, National Hellenic Research Foundation, 48 Vassileos Constantinou Avenue, 11635 Athens, Greece*

\*Corresponding authors:

[topper3@unm.edu](mailto:topper3@unm.edu) (B. Topper)

[cvars@uniwa.gr](mailto:cvars@uniwa.gr) (C.P.E. Varsamis)

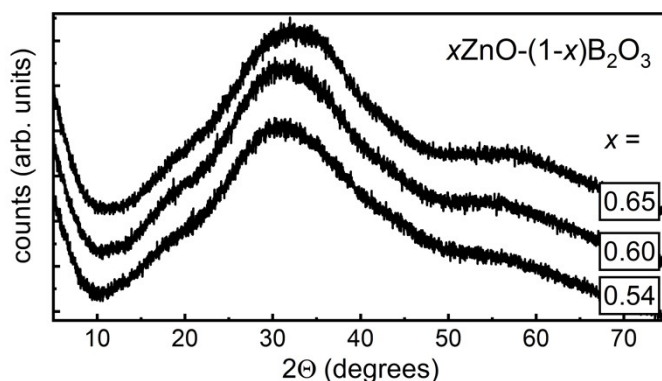


**Figure S1.** X-ray diffraction patterns for upper and lower ZnO limits of  $x\text{ZnO}-(1-x)\text{B}_2\text{O}_3$  glasses capable of being prepared in large sample sizes and cooled slowly without crystallizing.

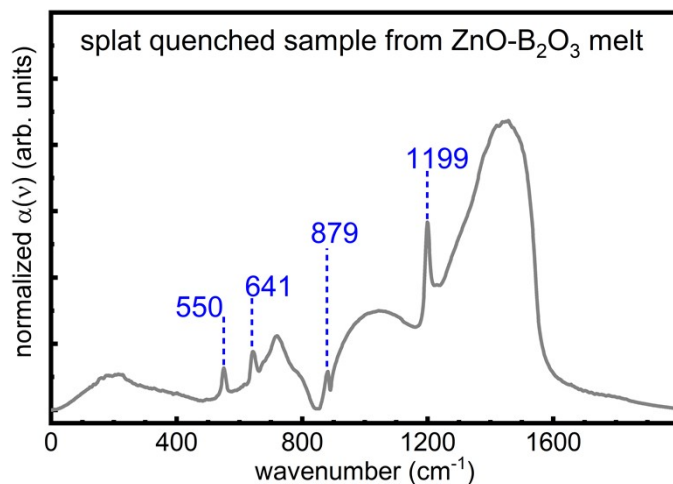


**Figure S2.** Infrared absorption coefficient spectrum measured from splat quenched  $x=0.50$  zinc borate glass. The vertical lines denote characteristic infrared activity of boric acid. The larger spot size of the infrared beam, relative to Raman measurements discussed in the main text, probes a larger sample area thus capturing both components of the phase separated sample.

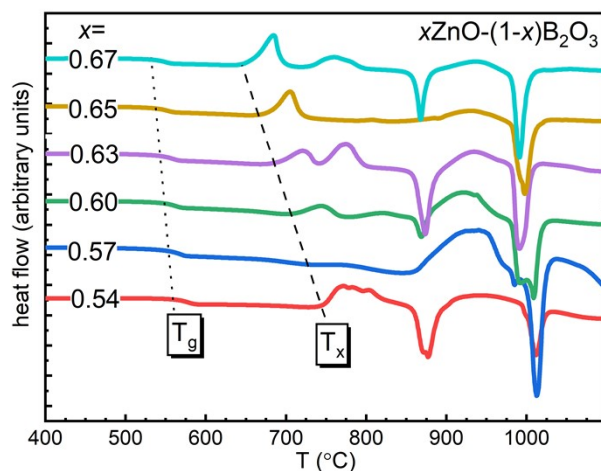


**Figure S3.** DSC scans for binary zinc borate glasses. The glass transition temperature trend is represented by the dotted line while the trend in the onset temperature of crystallization is depicted by the dashed line.

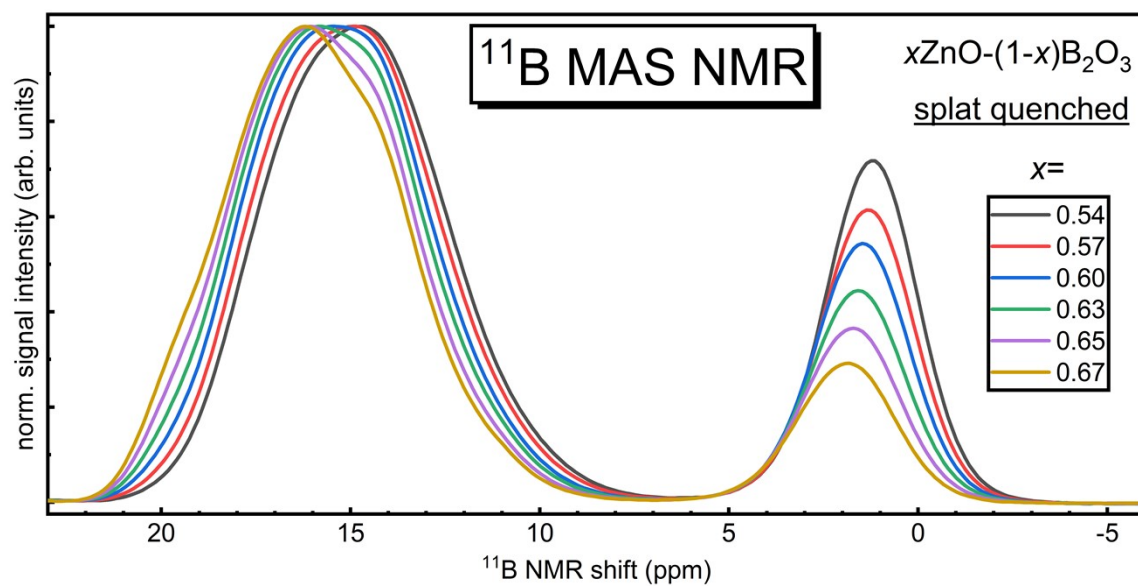


**Figure S4.**  $^{11}\text{B}$  MAS NMR spectra of binary zinc borates taken at 16.4 T on splat quenched glass samples.

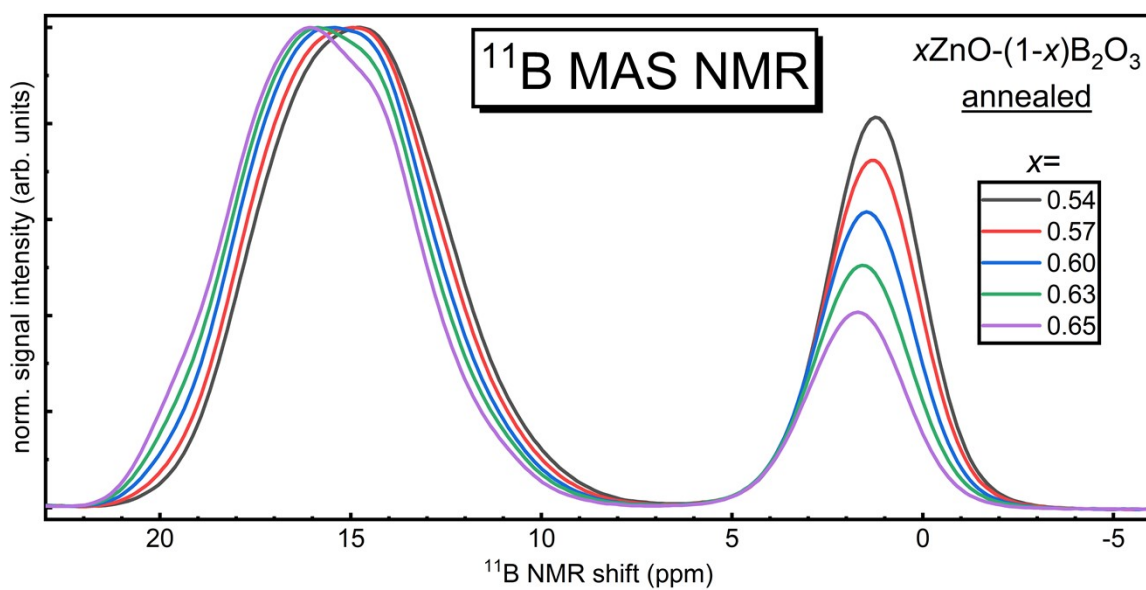


**Figure S5.**  $^{11}\text{B}$  MAS NMR spectra of binary zinc borates taken at 16.4 T on annealed glass samples.

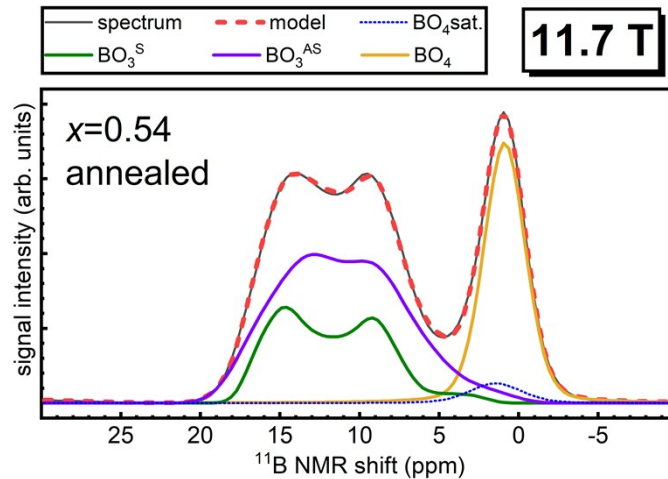


**Figure S6.**  $^{11}\text{B}$  MAS NMR spectra of annealed  $0.54\text{ZnO}-0.46\text{B}_2\text{O}_3$  glass measured at 11.7 T and fitted using results from higher field (16.4 T). The fit here gives 24.4%  $\text{B}_3^{\text{S}}$ , 48.2%  $\text{B}_3^{\text{AS}}$ , and 27.4%  $\text{B}_4$ .

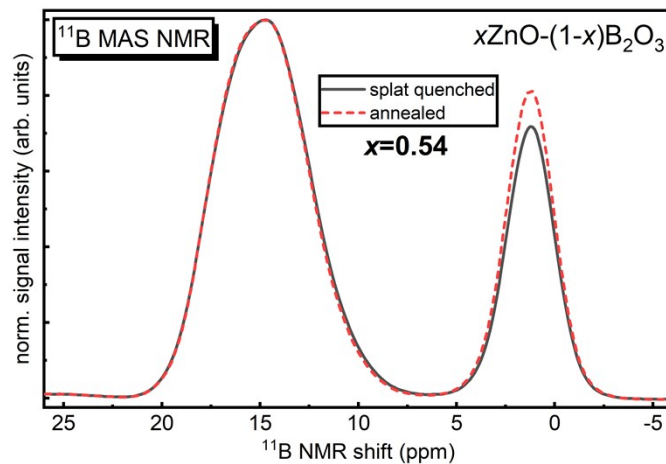


**Figure S7.**  $^{11}\text{B}$  MAS NMR spectra of  $0.54\text{ZnO}-0.46\text{B}_2\text{O}_3$  glass measured at 16.4 T for splat quenched (solid black) and annealed (dashed red) glasses.

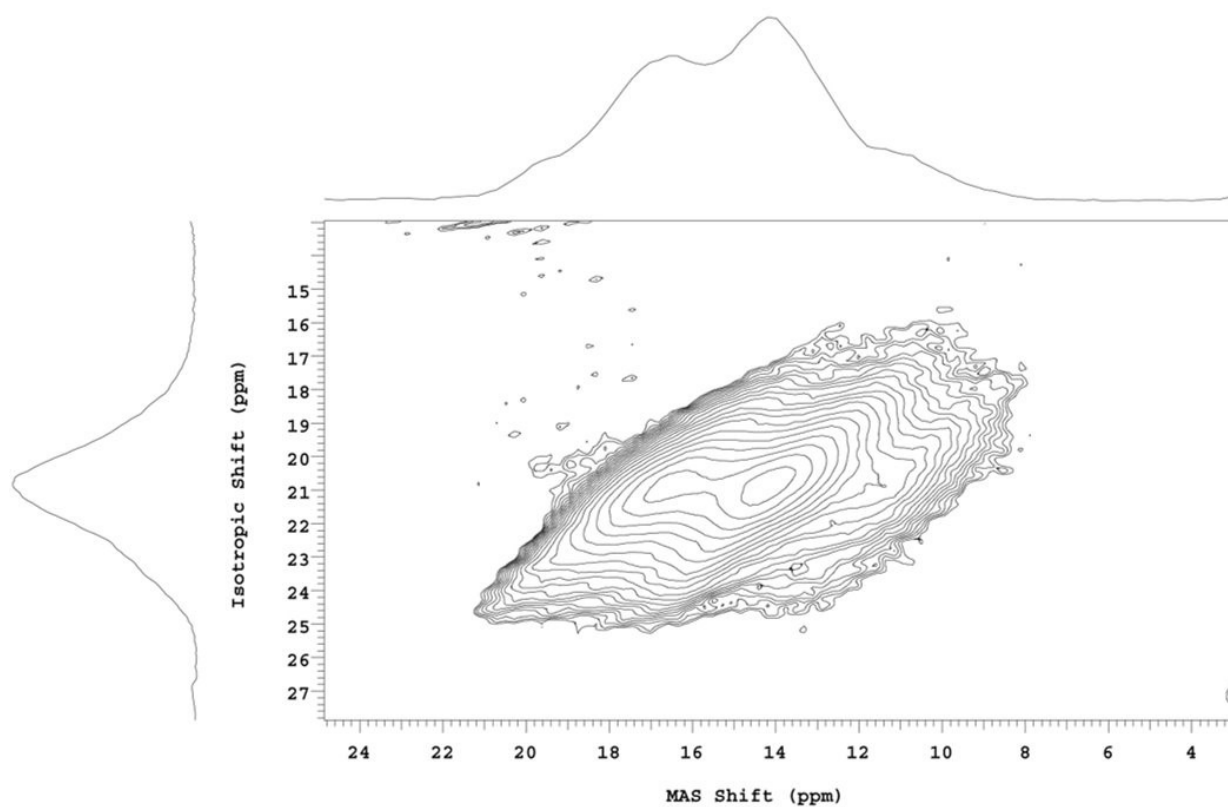


**Figure S8.**  $^{11}\text{B}$  3QMAS NMR measurement of splat quenched  $0.63\text{ZnO}-0.37\text{B}_2\text{O}_3$  glass measured at 16.4 T, showing only the spectral region for  $\text{BO}_3$ . It is difficult to see any distinction in the MAS lineshape (i.e. quadrupolar coupling asymmetry parameter,  $\eta$ ) for the different  $\text{BO}_3$  signals identified in the isotropic project (curve plotted to the left).